

Crystalline Boson Phases in Harmonic Traps: Beyond the Gross-Pitaevskii Mean Field

Igor Romanovsky, Constantine Yannouleas, and Uzi Landman

School of Physics, Georgia Institute of Technology, Atlanta, Georgia 30332-0430, USA

(Received 29 June 2004; published 1 December 2004)

Strongly-interacting bosons in two-dimensional harmonic traps are described through breaking of rotational symmetry at the Hartree-Fock level and subsequent symmetry restoration via projection techniques, thus incorporating correlations beyond the Gross-Pitaevskii (GP) solution. The bosons localize and form polygonal-ringlike crystalline patterns, both for a repulsive contact potential and a Coulomb interaction, as revealed via conditional-probability-distribution analysis. For neutral bosons, the total energy of the crystalline phase saturates in contrast to the GP solution, and its spatial extent becomes smaller than that of the GP condensate. For charged bosons, the total energy and dimensions approach the values of classical pointlike charges in their equilibrium configuration.

DOI: 10.1103/PhysRevLett.93.230405

PACS numbers: 03.75.Hh, 03.75.Nt

Bose-Einstein condensates (BECs) in harmonic traps [1] are normally associated with weakly interacting neutral atoms, and their physics is described adequately by the Gross-Pitaevskii (GP) mean-field theory [2]. Lately, however, experimental advances in controlling the interaction strength [3–6] permit the production of novel bosonic states in the regime of strong interparticle repulsions. Theoretical efforts motivated by this capability include studies of the Bose-Hubbard model [7,8], and investigations about the “fermionization” limit of a one-dimensional (1D) gas of trapped impenetrable bosons [9–11], often referred to as the Tonks-Girardeau (TG) regime [9,12]. In this Letter, we address the still open problem of strongly repelling (impenetrable) bosons in higher dimensions, and, in particular, in two dimensions (2D).

We describe the strongly repelling bosons through symmetry breaking at the Hartree-Fock (HF) mean-field level followed by post-Hartree-Fock symmetry restoration, thus incorporating correlations beyond the GP solution. This two-step method, which has not been applied yet to the bosonic many-body problem, has been shown to successfully describe strongly correlated electrons in 2D semiconductor quantum dots [13]. We focus here on results for 2D interacting bosons in a harmonic trap, with the extension to 3D systems being straightforward.

To illustrate our method, we consider systems with a few bosons. The method describes the transition from a BEC state to a crystalline phase, in which the trapped localized bosons form crystalline patterns. In 2D, these patterns are ringlike, both for a repulsive contact and a Coulomb interaction. At the mean-field level, these crystallites are static and are portrayed directly in the single-particle densities. After restoration of symmetry, the single-particle densities are rotationally symmetric, and thus the crystalline symmetry becomes “hidden”; however, it can be revealed in the conditional-probability distribution (CPD, anisotropic pair correlation), $P(\mathbf{r}, \mathbf{r}_0)$, which expresses the probability of finding a particle at \mathbf{r}

given that the “observer” (i.e., reference point) is riding on another particle at \mathbf{r}_0 [14].

Mean-field symmetry breaking for bosonic systems has been discussed earlier in the context of two-component condensates, where each species is associated with a different space orbital [15]. We consider here one species of bosons, but allow each particle to occupy a different space orbital $\phi_i(\mathbf{r}_i)$. The permanent $|\Phi_N\rangle = \text{Perm}[\phi_1(\mathbf{r}_1), \dots, \phi_N(\mathbf{r}_N)]$ serves as the many-body wave function of the *unrestricted* Bose-Hartree-Fock (UBHF) approximation. This wave function reduces to the Gross-Pitaevskii form with the *restriction* that all bosons occupy the same orbital $\phi_0(\mathbf{r})$, i.e., $|\Phi_N^{\text{GP}}\rangle = \prod_{i=1}^N \phi_0(\mathbf{r}_i)$, and $\phi_0(\mathbf{r})$ is determined self-consistently at the restricted Bose-Hartree-Fock (RBHF) level [16] via the equation [17] $[H_0(\mathbf{r}_1) + (N-1) \int d\mathbf{r}_2 \phi_0^*(\mathbf{r}_2) \times V(\mathbf{r}_1, \mathbf{r}_2) \phi_0(\mathbf{r}_2)] \phi_0(\mathbf{r}_1) = \epsilon_0 \phi_0(\mathbf{r}_1)$. Here $V(\mathbf{r}_1, \mathbf{r}_2)$ is the two-body repulsive interaction, which can be either a long-range Coulomb force, $V_C = Z^2 e^2 / (\kappa |\mathbf{r}_1 - \mathbf{r}_2|)$, for charged bosons or a contact potential, $V_\delta = g \delta(\mathbf{r}_1 - \mathbf{r}_2)$, for neutral bosons. The single-particle Hamiltonian is given by $H_0(\mathbf{r}) = -\hbar^2 \nabla^2 / (2m) + m \omega_0^2 \mathbf{r}^2 / 2$, where ω_0 characterizes the harmonic confinement.

First step: Symmetry-breaking.—Going beyond the GP approach to the *unrestricted* Hartree-Fock level (i.e., using the permanent $|\Phi_N\rangle$) results in a set of UBHF equations with a higher complexity than that encountered in electronic structure problems [13(a)]. Consequently, we simplify the UBHF problem by considering explicit analytic expressions for the space orbitals $\phi_i(\mathbf{r}_i)$. In particular, since *the bosons must avoid occupying the same position in space in order to minimize their mutual repulsion*, we take all the orbitals to be of the form of displaced Gaussians [18], namely, $\phi_i(\mathbf{r}_i) = \pi^{-1/2} \sigma^{-1} \times \exp[-(\mathbf{r}_i - \mathbf{a}_i)^2 / (2\sigma^2)]$. The positions \mathbf{a}_i describe the vertices of concentric regular polygons, with both the width σ and the radius $a = |\mathbf{a}_i|$ of the regular polygons determined variationally through minimization of the total energy $E_{\text{UBHF}} = \langle \Phi_N | H | \Phi_N \rangle / \langle \Phi_N | \Phi_N \rangle$, where

$H = \sum_{i=1}^N H_0(\mathbf{r}_i) + \sum_{i<j}^N V(\mathbf{r}_i, \mathbf{r}_j)$ is the many-body Hamiltonian.

With the above choice of localized orbitals, the unrestricted permanent $|\Phi_N\rangle$ breaks the continuous rotational symmetry. However, for both the cases of a contact potential and a Coulomb force, the resulting energy gain becomes substantial for stronger repulsion. Controlling this energy gain (the strength of correlations) is the ratio R between the strength of the repulsive potential and the zero-point kinetic energy. Specifically, for a 2D trap, one has $R_\delta = gm/(\pi\hbar^2)$ for a contact potential and $R_W = Z^2 e^2/(\hbar\omega_0 l_0)$ for a Coulomb force, with $l_0 = \sqrt{\hbar/(m\omega_0)}$ being the characteristic harmonic-oscillator length. (The subscript W in the case of a Coulomb force stands for ‘‘Wigner’’, since the Coulomb crystallites in harmonic traps are finite-size analogs of the bulk Wigner crystal [19].)

In Fig. 1, we display as a function of the parameters R_δ (a) and R_W (b), respectively, the total energies for $N = 6$ bosons calculated at several levels of approximation. In both cases the lowest UBHF energies correspond to a (1, 5) crystalline configuration, namely, one boson is at the center and the rest form a regular pentagon of radius a . Observe that the GP total energies are slightly lower than the $E_{\text{RBHF}}^{\text{Gauss}}$ ones; however, both exhibit an unphysical behavior since they diverge as $R_\delta \rightarrow \infty$. This behavior

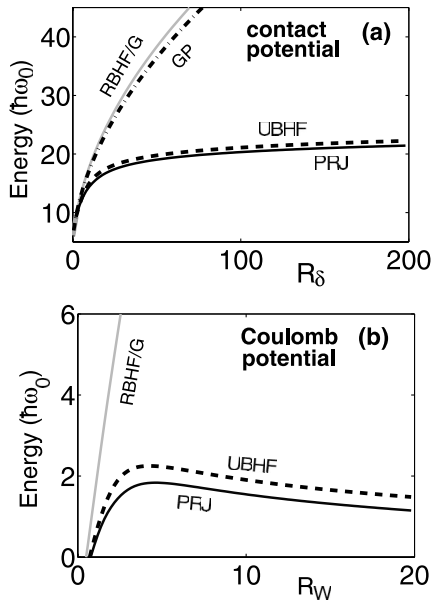


FIG. 1. Total energies as a function (a) of R_δ and (b) of R_W for various approximation levels, calculated for $N = 6$ harmonically confined 2D bosons in the (1, 5) lowest-energy configuration. Notation: RBHF/G—Restricted Bose-Hartree-Fock (RBHF) energy, $E_{\text{RBHF}}^{\text{Gauss}}$, with the common orbital $\phi_0(\mathbf{r})$ approximated by a Gaussian centered at the trap origin; GP—the Gross-Pitaevskii energy; PRJ—the energy of the symmetry-restored state obtained via projection of the (unrestricted) UBHF state. Energies in units of $\hbar\omega_0$.

contrasts sharply with that of the unrestricted Hartree-Fock energies, E_{UBHF} and those of the projected (PRJ) states (see below), which saturate as $R_\delta \rightarrow \infty$; in fact, a value close to saturation is achieved already for $R_\delta(R_W) \sim 10$. We have checked that for all cases with $N = 2-7$, the total energies exhibit a similar behavior. For a repulsive contact potential, the saturation of the UBHF energies is associated with the ability of the trapped bosons (independent of N) to minimize their mutual repulsion by occupying different positions in space, and this is one of our central results. For $N = 2$, the two bosons localize at a distance $2a$ apart to form an antipodal dimer. For $N \leq 5$ the preferred UBHF crystalline arrangement is a single ring with no boson at the center [usually denoted as $(0, N)$]. $N = 6$ is the first case having one boson at the center [designated as $(1, N - 1)$], and the $(0, 6)$ arrangement is a higher energy isomer.

The saturation found here for 2D trapped bosons interacting through strong repelling contact potentials is an illustration of the fermionization analogies that appear in strongly correlated systems in all three dimensionalities. Indeed such energy saturation has been shown for the TG 1D gas [9,12], and has also been discussed for certain 3D systems (i.e., three trapped bosons [20] and an infinite boson gas [21]). Saturation of the energy and the length of the trapped atom cloud (and thus of the interparticle distance) has been measured recently for the 1D TG gas (see, in particular, Fig. 3 and Fig. 4 in Ref. [6] and compare to the similar trends predicted here for the 2D case in Fig. 1 and Fig. 2).

For the Coulomb potential [see Fig. 1(b)], the displayed total energies have been referenced to the classical energy E_C^{cl} [22] (plus the zero-point energy) of six trapped point charges in their (1, 5) equilibrium configuration, since the total energy of a Wigner crystallite (independently of whether it consists of bosons or fermions) is expected to approach E_C^{cl} as $R_W \rightarrow \infty$. We see again that the $E_{\text{RBHF}}^{\text{Gauss}}$ energies (one common Gaussian orbital) diverge as $R_W \rightarrow \infty$. In contrast, the unrestricted HF energies E_{UBHF} remain finite and approach slowly E_C^{cl} as $R_W \rightarrow \infty$. A similar behavior is exhibited by the total energies for all $N = 2-7$ cases of charged bosons.

In Fig. 2, we display for the $N = 6$ bosons the radii of the polygonal rings a and widths σ of the Gaussian orbitals obtained in various approximations, as a function of R_δ (a) and R_W (b). For the contact potential, in the RBHF/Gaussian approximation we find that $a = 0$ and the width (marked as RBHF/G in Fig. 2) keeps increasing continuously as $R_\delta \rightarrow \infty$ (this reflects the unsuccessful attempt of the common orbital to minimize the mutual repulsion between the bosons by spreading out as far as possible). In contrast, the unrestricted widths σ_{UBHF} associated with the displaced Gaussian orbitals (that correspond to a lower total energy, see Fig. 1) saturate to a constant value. Similar behaviors are also exhibited by $\sigma_{\text{RBHF}}^{\text{Gauss}}$ and σ_{UBHF} in the case of a Coulomb force [see Fig. 2(b)].

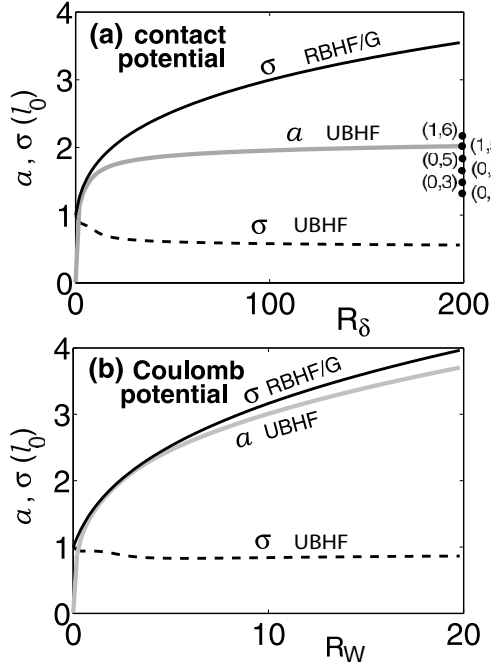


FIG. 2. Variationally determined widths (σ) and ring radii (a) for $N = 6$ harmonically confined 2D bosons as a function of (a) R_δ and (b) R_W , obtained according to the various approximations (as marked in the figure, see also caption of Fig. 1). The saturation values of a of the lowest-energy configuration for $2 \leq N \leq 7$ are on the right in (a). Lengths are in units of l_0 . For the UBHF case [displaying a (1, 5) crystallite] the interparticle distance on the pentagonal shell is $d = ((5 - 5^{1/2})/2)^{1/2}a \approx 1.176a$, showing the same saturation trend as the radius a .

The radii a associated with the pentagonal ring of localized orbitals, however, exhibit a different behavior depending on whether the repulsive potential is a contact or a Coulomb one. Indeed, in the Coulomb case, the radii a_{UBHF} keep increasing with R_W , approaching the equilibrium radius $a_C^{\text{cl}} = 1.334l_0R_W^{1/3}$ of six Ze classical point charges in a harmonic trap in the (1, 5) configuration [22]. In contrast, for a repulsive contact potential, the radii a_{UBHF} saturate to a constant value $\approx 2l_0$. The dependence of the saturation values of a on N (for $3 \leq N \leq 7$) for the lowest-energy configurations is shown on the right in Fig. 2(a). The different behavior of the boson positions in the UBHF crystallite is a natural consequence of the long-range character of the Coulomb potential versus the short-range contact potential.

Second step: Restoration of broken symmetry.— Although the optimized UBHF permanent $|\Phi_N\rangle$ performs exceptionally well regarding the total energies of the trapped bosons, in particular, in comparison to the restricted wave functions (e.g., the GP ansatz), it is still incomplete. Indeed, due to its localized orbitals, $|\Phi_N\rangle$ does not preserve the circular (rotational) symmetry of the 2D many-body Hamiltonian H . Instead, it exhibits a lower point-group symmetry, i.e., a C_2 symmetry for $N = 2$ and a C_5 one for $N = 6$ (see below). As a result,

$|\Phi_N\rangle$ does not have a good total angular momentum. This is resolved through a post-Hartree-Fock step of *restoration* of broken symmetries via projection techniques [13(b),22], yielding a new wave function $|\Psi_{N,L}^{\text{PRJ}}\rangle$ [23] with a definite angular momentum L . Here, we focus on the properties of the ground state, i.e., $L = 0$; the corresponding energy is E_0^{PRJ} .

For $N = 6$ 2D bosons, Fig. 1 shows that the E_0^{PRJ} energies share with the UBHF ones the saturation property for the case of a contact-potential repulsion, as well as the property of converging to E_C^{cl} as $R_W \rightarrow \infty$ for the case of a Coulomb repulsion. In both cases, however, the projections bring further lowering [24] of the total energies compared to the UBHF ones. Thus, for strong interactions (large values of R_δ or R_W) the restoration-of-broken-symmetry step yields an excellent approximation of both the exact many-body wave function and the exact total energy [25].

The transformations of the single-particle densities (displayed in Fig. 3 for $N = 6$ neutral bosons interacting via a contact potential and $R_\delta = 25$) obtained from application of the successive approximations provide an illustration of the two-step method of symmetry breaking with subsequent symmetry restoration. Indeed, the GP single-particle density [Fig. 3(a)] is circularly symmetric, but the UBHF one [Fig. 3(b)] explicitly exhibits a (1, 5) crystalline configuration. After symmetry restoration [Fig. 3(c)], the circular symmetry is reestablished, but the single-particle density is radially modulated unlike the GP density. In addition, the crystalline structure in the projected wave function is now hidden; however, it can be revealed through the use of the CPD [14] [see Fig. 3(d)], which resembles the (crystalline) UBHF single-particle

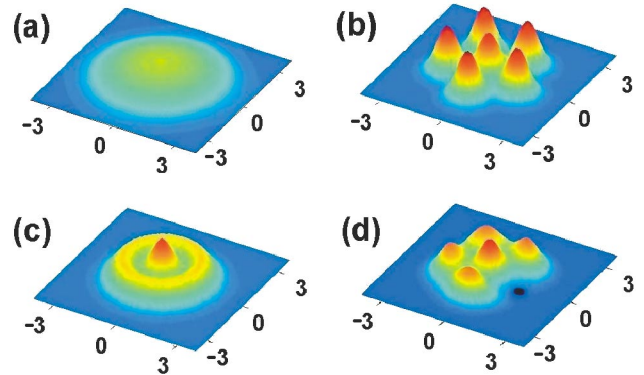


FIG. 3 (color). (a-c) Single-particle densities for $N = 6$ 2D harmonically trapped neutral bosons with a contact interaction and $R_\delta = 25$. (a) The single-orbital self-consistent GP case. (b) The symmetry broken UBHF case (static crystallite). (c) The projected (symmetry-restored) wave function, see Ref. [23] case (collectively fluctuating crystallite). The crystalline structure of the outer ring in this last case is hidden, but it is revealed in the conditional-probability distribution [14] displayed in (d), where the observation point is denoted by a black dot (on the right). Lengths in units of l_0 .

density, but with one of the humps on the outer ring missing (where the observer is located). In particular, $P(\mathbf{r}_0, \mathbf{r}_0) \approx 0$ and the boson associated with the observer is surrounded by a “hole” similar to the exchange-correlation hole in electronic systems. This is another manifestation of the fermionization of the strongly repelling 2D bosons. However, here as in the 1D TG case [9,12], the vanishing of $P(\mathbf{r}_0, \mathbf{r}_0)$ results from the impenetrability of the bosons. For the GP condensate, the CPD is independent of \mathbf{r}_0 , i.e., $P_{\text{GP}}(\mathbf{r}, \mathbf{r}_0) \propto |\phi_0(\mathbf{r})|^2$, reflecting the absence of any space correlations.

It is of importance to observe that the radius of the BEC [GP case, Fig. 3(a)] is significantly larger than the actual radius of the strongly-interacting crystalline phase [projected wave function, Fig. 3(c)]. This is because the extent of the crystalline phase saturates, while that of the GP condensate grows with no bounds as $R_\delta \rightarrow \infty$. Such dissimilarity in size (between the condensate and the strongly-interacting phase) has been also predicted [10] for the trapped 1D Tonks-Girardeau gas and indeed observed experimentally [6]. In addition, the 2D single-particle momentum distributions for neutral bosons have a one-hump shape with a maximum at the origin (a behavior exhibited also by the trapped 1D TG gas). The width of these momentum distributions versus R_δ increases and saturates to a finite value, while that of the GP solution vanishes as $R_\delta \rightarrow \infty$.

In conclusion, we provided a solution to strongly repelling bosons in 2D harmonic traps using a two-step method of breaking of rotational symmetry at the unrestricted Bose-Hartree-Fock level and of subsequent symmetry restoration. This method yields substantially lower total energies compared to the GP solution, through the inclusion of correlations beyond the single-orbital Bose-Einstein condensate. We find that the bosons become localized and form crystalline patterns made of concentric polygonal rings, both for a repulsive contact and a Coulomb interaction. For neutral bosons the total energy of the crystalline phase saturates with increasing strength of the repulsion, in contrast to the GP condensate whose energy diverges. Furthermore, the spatial extent saturates and becomes smaller than that of the GP condensate, which grows without limit. For charged bosons, the total energy and spatial extent of the crystalline phase approach the classical values of pointlike charges in their equilibrium configuration as $R_W \rightarrow \infty$. In light of the above, we trust that our predictions will provide the impetus for experimental efforts to access the regime of strongly repelling bosons in two dimensions. To this end we anticipate that extensions of methodologies developed for the recent realization of the Tonks-Girardeau regime in 1D (using a finite small number of trapped ^{87}Rb and optical lattices, with a demonstrated wide variation of R_δ from 5 to 200 [5] and from 1 to 5 [6]) will prove most promising. Control of the interaction strength via the use of the Feshbach resonance may also be considered [3].

This research is supported by the U.S. D.O.E. (Grant No. FG05-86ER45234) and by the NSF.

-
- [1] E. A. Cornell and C. E. Wieman, *Rev. Mod. Phys.* **74**, 875 (2002); W. Ketterle, *Rev. Mod. Phys.* **74**, 1131 (2002).
 - [2] F. Dalfovo *et al.*, *Rev. Mod. Phys.* **71**, 463 (1999).
 - [3] S. L. Cornish *et al.*, *Phys. Rev. Lett.* **85**, 1795 (2000).
 - [4] M. Greiner *et al.*, *Nature (London)* **415**, 39 (2002).
 - [5] B. Paredes *et al.*, *Nature (London)* **429**, 277 (2004).
 - [6] G. T. Kinoshita, T. Wenger, and D. S. Weiss, *Science* **305**, 1125 (2004), published after the submission of this Letter.
 - [7] D. Jaksch *et al.*, *Phys. Rev. Lett.* **81**, 3108 (1998).
 - [8] See, e.g., O. I. Motrunich and T. Senthil, *Phys. Rev. Lett.* **89**, 277004 (2002).
 - [9] M. D. Girardeau and E. M. Wright, *Laser Phys.* **12**, 8 (2002).
 - [10] V. Dunjko *et al.*, *Phys. Rev. Lett.* **86**, 5413 (2001).
 - [11] See, e.g., G. E. Astrakharchik and S. Giorgini, *Phys. Rev. A* **66**, 053614 (2002).
 - [12] M. Girardeau, *J. Math. Phys. (N.Y.)* **1**, 516 (1960).
 - [13] (a) C. Yannouleas and U. Landman, *Phys. Rev. Lett.* **82**, 5325 (1999); **85**, 2220(E) (2000); *Phys. Rev. B* **68**, 035325 (2003); (b) *J. Phys. Condens. Matter* **14**, L591 (2002); *Phys. Rev. B* **68**, 035326 (2003).
 - [14] C. Yannouleas and U. Landman, *Phys. Rev. Lett.* **85**, 1726 (2000); *cond-mat/0401610*.
 - [15] P. Öhberg and S. Stenholm, *Phys. Rev. A* **57**, 1272 (1998); B. D. Esry, and C. H. Greene, *Phys. Rev. A* **59**, 1457 (1999).
 - [16] For the corresponding Hartree-Fock terminology for fermions, see Ref. [13(a)].
 - [17] B. D. Esry, *Phys. Rev. A* **55**, 1147 (1997).
 - [18] For strongly correlated electrons in parabolic quantum dots the Gaussian form is adequate in most cases, leading to formation of electron crystallites [13] (Wigner molecules).
 - [19] E. Wigner, *Phys. Rev.* **46**, 1002 (1934).
 - [20] D. Blume and C. H. Greene, *Phys. Rev. A* **66**, 013601 (2002).
 - [21] H. Heiselberg, *J. Phys. B* **37**, S141 (2004).
 - [22] C. Yannouleas and U. Landman, *Phys. Rev. B* **69**, 113306 (2004).
 - [23] The projected multipermanent wave function can be written as $2\pi|\Psi_{N,L}^{\text{PRJ}}\rangle = \int_0^{2\pi} d\gamma |\Phi_N(\gamma)\rangle \exp(i\gamma L)$, where $|\Phi_N(\gamma)\rangle$ is the original UBHF permanent having each localized orbital rotated by an azimuthal angle γ , with L being the total angular momentum. The projection yields wave functions for a whole rotational band. The projected ground-state ($L = 0$) energy is given by $E_0^{\text{PRJ}} = \langle \Psi_{N,0}^{\text{PRJ}} | H | \Psi_{N,0}^{\text{PRJ}} \rangle / \langle \Psi_{N,0}^{\text{PRJ}} | \Psi_{N,0}^{\text{PRJ}} \rangle$.
 - [24] The projected ground state is always lower in energy than the original broken-symmetry one [P.-O. Löwdin, *Rev. Mod. Phys.* **34**, 520 (1962), in particular, Sect. 3].
 - [25] Energies calculated from the *symmetry-breaking* mean-field approach (i.e., the UBHF energies and projections thereof) improve relative to the exact energies for larger N ; see, P. Ring and P. Schuck, *The Nuclear Many-Body Problem* (Springer-Verlag, New York, 1980), Chap. 11.